

Muneto Nitta¹ · Minoru Eto² · Mattia
Cipriani³

Vortex molecules in Bose-Einstein condensates

XX.XX.2013

Keywords Bose-Einstein condensates, multi-component, vortices, fractional vortices, vortex molecules, graph theory

Abstract Stable vortex dimers are known to exist in coherently coupled two component Bose-Einstein condensates (BECs). We construct stable vortex trimers in three component BECs and find that the shape can be controlled by changing the internal coherent (Rabi) couplings. Stable vortex N -omers are also constructed in coherently coupled N -component BECs. We classify all possible N -omers in terms of the mathematical graph theory. Next, we study effects of the Rabi coupling in vortex lattices in two-component BECs. We find how the vortex lattices without the Rabi coupling known before are connected to the Abrikosov lattice of integer vortices with increasing the Rabi coupling. In this process, vortex dimers change their partners in various ways at large couplings. We then find that the Abrikosov lattices are robust in three-component BECs.

PACS numbers: 03.75.Lm, 03.75.Mn, 11.25.Uv, 67.85.Fg

1 Introduction

The study of Bose-Einstein condensates (BECs) can provide an ideal opportunity to examine the dynamics of exotic vortices because these vortices can theoretically be explained via a quantitative description using the mean field theory by the Gross-Pitaevski (GP) equation and further, the vortices can be experimentally controlled to a large degree. Vortices in multi-component BECs have been realized experimentally^{1,2}, and the structures of vortices in spinor BECs^{3,4,5}

1: Department of Physics, and Research and Education Center for Natural Sciences, Keio University, Hiyoshi 4-1-1, Yokohama, Kanagawa 223-8521, Japan
E-mail: nitta@phys-h.keio.ac.jp

2: Department of Physics, Yamagata University, Yamagata 990-8560, Japan

3: University of Pisa, Department of Physics "E. Fermi", INFN, Largo Bruno Pontecorvo 7, 56127, Italy

and in mixtures of multiple species and/or multiple hyperfine states of the same atom^{6,7,8,9,10,11,12,13,14,15,16,17,18} are considerably richer than those formed of single components; one fascinating feature in such cases is that vortices are fractionally quantized, and the other is that sets of fractional vortices constitute vortex molecules. In the case of multiple hyperfine spin states of BECs, internal coherent (Rabi) couplings between multiple components can be introduced by Rabi oscillations, similar to Josephson couplings in multi-gap superconductors. As in two-gap superconductors¹⁹, a sine-Gordon domain wall of the phase difference of two components (phase soliton) appears²⁰. In this light, the advantages of BECs are that Rabi coupling can be tuned experimentally and that in contrast to two-gap superconductors^{21,22}, a vortex dimer, that is two fractional vortices connected by a phase soliton, can exist stably because a repulsion between two fractional vortices¹¹ is sufficiently strong in the absence of the Meissner effect, to be balanced with the tension of a sine-Gordon domain wall connecting them⁸.

Recently, we have observed stable-vortex trimers in three-component BECs, and we have shown that the shape and the size of the molecule can be controlled by varying the strength of the Rabi couplings¹⁵. We have further constructed stable-vortex N -omers, that is, molecules made of N fractional vortices in N -component BECs, where each condensate wave function has a nontrivial winding number around one of the N fractional vortices¹⁶. N -omers with $N \geq 3$ exhibit several novel properties that dimers do not possess, that is, the existence of chirality pairs and metastable states such as twist, holding, and capture, which are properties exhibited by chemical molecules. The mathematical graph theory is useful to classify the vortex N -omers whose number exponentially increases as N increases. All possible graphs have been constructed for $N = 3, 4, 5$ by imaginary time propagation¹⁶ with the phase winding and a constant density fixed at the boundaries, thereby our results imply that the vortex N -omers are formed in rotating BECs.

The Rabi coupling in vortex lattices in two-component BECs under rotation has been studied systematically¹⁷. The triangular and square vortex lattices are connected to the Abrikosov lattices of integer vortices at the strong Rabi coupling, while in the intermediate Rabi couplings, we find that vortices change their partners in various ways depending on the inter-component coupling. Vortex lattices in a three-component BEC with three kinds of fractional vortices winding one of three components have been studied recently¹⁸. We always find triangular ordered vortex lattices, where three kind of fractional vortices are placed in order without defects.

2 N -component BECs

We consider coherently coupled miscible N -component BECs of atoms with mass m , described by the condensate wave functions Ψ_i ($i = 1, 2, \dots, N$) with the GP energy functional

$$E = \sum_{i,j=1}^N \int d^2x \left(\frac{\hbar^2}{2m} \left| \left(-i\nabla - \frac{m}{\hbar} \boldsymbol{\Omega} \times \mathbf{r} \right) \Psi_i \right|^2 \delta_{ij} + \frac{g_{ij}}{2} |\Psi_i|^2 |\Psi_j|^2 + (V_{\text{eff.}} - \mu_i |\Psi_i|^2) \delta_{ij} - \omega_{ij} \Psi_i^* \Psi_j \right), \quad (1)$$

where atom-atom interactions are characterized by the coupling constants $g_{ij} = 4\pi\hbar^2 a_{ij}/m$ with s-wave scattering lengths a_{ij} , μ_i denotes the chemical potential, and $\omega_{ij} = \omega_{ji}$ ($\omega_{ii} = 0$) denotes the internal coherent coupling due to Rabi oscillations between the i -th and j -th components. Ω is the rotation frequency of the system, and $V_{\text{eff.}} = V_{\text{ex.}} - m\Omega^2 r^2/2$ is the effective trapping potential of the external potential $V_{\text{ex.}}$ combined with the centrifugal potential. We mainly consider the case where $g_{ii} \equiv g$, and $\mu_i \equiv \mu$, and $g_{ij} \equiv \tilde{g}$ ($i \neq j$). It is straightforward to consider the general case but all the results below are essentially unchanged from our simplest choice. We mostly consider the miscible case $g > \tilde{g}$. The symmetry of the Hamiltonian depends on the coupling constants:

$$\begin{cases} U(N), & g = \tilde{g}, & \omega_{ij} = 0, \\ U(1)^N, & g \neq \tilde{g}, & \omega_{ij} = 0, \\ U(1), & g \neq \tilde{g}, & \omega_{ij} \neq 0 \end{cases} \quad (2)$$

Let us consider an infinite uniform system with $\Omega = 0$ and $V_{\text{eff.}} = 0$. When all the internal coherent couplings are equal *i.e.*, $\omega_{ij} = \omega$, the condensations of the ground state are

$$|\Psi_i| = v \equiv \sqrt{\frac{\mu + (N-1)\omega}{g + (N-1)\tilde{g}}}, \quad (3)$$

with $i = 1, 2, \dots, N$. These amplitudes are modified in the case $\omega_{ij} \neq \omega_{j'j'}$, and one should solve the variational problem $\delta E / \delta \Psi_i = 0$ to determine $v_i = |\Psi_i|$.

As long as the internal coherent couplings $|\omega_{ij}|$ are maintained sufficiently small with respect to the other couplings (we choose $g \sim \tilde{g} = \mathcal{O}(10^3)$, $\mu = \mathcal{O}(10^2)$, and $\omega = \mathcal{O}(10^{-2})$), the symmetries (2) are nearly intact. These symmetries are spontaneously broken in the ground state. Consequently, vortices that are quite different for $g = \tilde{g}$ and $g > \tilde{g}$ can appear.

The internal coherent couplings $-\omega_{ij}\Psi_i^*\Psi_j = -2v_i v_j \omega_{ij} \cos(\theta_i - \theta_j)$, with $\theta_i = \arg \Psi_i$, give gaps to the Leggett modes $\theta_i - \theta_j$. If we approximate the amplitudes of the condensate wave functions to be constant, $|\Psi_i| = v_i e^{i\theta_i}$, the truncated energy functional is obtained as

$$\mathcal{E}_{\text{phase}} = \sum_{i=1}^N \frac{\hbar^2}{2m} (\nabla \theta_i)^2 - 2 \sum_{i>j}^N \omega_{ij} v_i v_j \cos(\theta_i - \theta_j). \quad (4)$$

For $\omega_{ij} > 0$, all the phases θ_i and θ_j coincide, *i.e.*, $\theta_i = \theta_j$ in the ground state. This model allows sine-Gordon domain walls (phase solitons). For two components $N = 2$, the conventional sine-Gordon domain walls are allowed²⁰. The same phase solitons were also predicted in two-gap superconductors¹⁹. For higher N , domain wall junctions may exist, but no analytic solutions are available.

3 Vortex molecules

In this section, we discuss one integer vortex which is split into fractional vortices. For this purpose, it is enough to consider an infinite uniform system with $\Omega = 0$ and $V_{\text{eff.}} = 0$ with the boundary condition for the phase winding.

3.1 Fractional vortices

First, let us consider the case that all ω_{ij} 's are zero. A vortex winding around only the i -th component ($i = 1, \dots, N$), $\Psi_i = v_i \rho(r) e^{i\theta}$, in polar coordinates r and θ , with the other components almost constant, is fractionally quantized as

$$\oint d\mathbf{r} \cdot \mathbf{v}_s = \frac{v_i^2}{\sum_i v_i^2} \frac{h}{m}, \quad (5)$$

with the superfluid velocity \mathbf{v}_s , and it is stable. We label it by an N -vector $(0, \dots, 1, \dots, 0)$ where i -th component is 1. The interaction between two vortices in the same component separated by the distance R is $F \sim 1/R$ as the same as that between two integer vortices in the scalar BEC, while the interaction between vortices in different components, say $(1, 0)$ and $(0, 1)$, is $F \sim g_{12}(\log R/\xi - 1/2)/R^3$, which is repulsive in our case of $g_{12} > 0$ ¹¹.

For $g = \bar{g}$, an axisymmetric giant vortex appears. This can be interpreted as a $\mathbb{C}P^{N-1}$ skyrmion¹⁶. On the other hand, for the miscible case with $g > \bar{g}$, there appear N fractional vortices associated with the broken $U(1)^N$ symmetry, which are connected by domain walls, thereby resulting in molecules with N vortices. The reduced energy functional in Eq. (4) shows that $N - 1$ domain walls are attached to the i -th vortex in the direction $\theta_i = \theta_j$. Therefore, this vortex cannot remain stable in an isolated state, and it must be connected to the boundary or to vortices winding around the other components forming the molecules.

3.2 Vortex dimers

Vortex dimers are molecules of two vortices appearing in two-component BECs⁸. Vortices winding around the first and the second components denoted by $(1, 0)$ and $(0, 1)$, respectively, are connected by a sine-Gordon domain wall²⁰. To see this, we note that the reduced energy functional is

$$\mathcal{E}_{\text{phase}} = \frac{\hbar^2}{4m} [\nabla(\theta_1 + \theta_2)]^2 + \frac{\hbar^2}{4m} [\nabla(\theta_1 - \theta_2)]^2 - 2\omega_{12}v_1v_2 \cos(\theta_1 - \theta_2). \quad (6)$$

We see that the overall phase $\theta_1 + \theta_2$ decouples and the phase difference $\theta_1 - \theta_2$ becomes the sine-Gordon model. Let us place the $(1, 0)$ and $(0, 1)$ vortices at P_1 and P_2 , respectively in Fig. 1. The $(1, 0)$ and $(0, 1)$ vortices are enclosed by the paths $b_1 + r$ and $b_2 - r$, respectively. Interpreting the label (a, b) as a generator acting as $(\Psi_1, \Psi_2) \rightarrow (\Psi_1 e^{ia\alpha}, \Psi_2 e^{ib\alpha})$, we decompose the generators $(1, 0)$ and $(0, 1)$ of vortices as

$$(1, 0) = \frac{1}{2}(1, 1) + \frac{1}{2}(1, -1), \quad (0, 1) = \frac{1}{2}(1, 1) - \frac{1}{2}(1, -1). \quad (7)$$

Since the total configuration has unit winding for the overall phase (gauge), the paths b_1 and b_2 correspond to the half windings generated by $(1, 1)$. Then, the other generator $(1, -1)$ acts along the path r :

$$\Psi_1(x=0, y) = e^{i\pi g(y)} |\Psi_1|, \quad \Psi_2(x=0, y) = e^{-i\pi g(y)} |\Psi_2|, \quad (8)$$

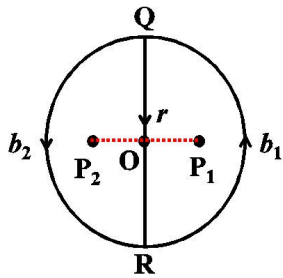


Fig. 1 The $(1,0)$, and $(0,1)$ vortices are placed at P_1, P_2 , respectively. b_i ($i = 1, 2$) correspond to $1/2$ circles at the boundary at spatial infinities, and r is the path connecting Q and R passing through the origin O . The $(1,0)$ and $(0,1)$ vortices are encircled by $b_1 + r$ and $b_2 - r$, respectively.

with monotonically increasing function $g(y)$ with the boundary conditions $g(y \rightarrow -\infty) = 0$ and $g(y \rightarrow \infty) = 1$. We find that the phase difference $\theta_1 - \theta_2$ changes by 2π along the path $-r$ and that a sine-Gordon domain wall exists on the path due to the potential term $V = 2\omega_{12}v_1v_2 \cos(\theta_1 - \theta_2)$ in (6). This domain wall connects the two fractional vortices.

In order to have a stable configuration, we need $g_{12} > 0$ so that two vortices repel each other for $\omega_{12} = 0$. For $\omega_{12} \neq 0$, the domain wall tension can be balanced with the repulsion between them, to yield a stable configuration. Numerical solutions of stable vortex dimers were obtained in Ref.⁸.

Vortex dimers were also proposed in two-gap superconductors²¹. However, in this case, the gauge symmetry is local. Consequently, the repulsion between $(1,0)$ and $(0,1)$ vortices are exponentially suppressed by the Meissner effect and cannot be balanced with a constant force of the domain wall tension (confinement). Instead, the deconfinement mechanism similar to the Berezinskii-Kosterlitz-Thouless transition at finite temperature was proposed²².

3.3 Vortex trimers

Three-component BECs admit vortex trimers, molecules of three vortices labeled as $(1,0,0)$, $(0,1,0)$, and $(0,0,1)$, winding around the first, second, and third component by 2π , respectively. The energy of each vortex is logarithmically divergent when $\omega_{ij} = 0$ and linearly divergent when $\omega_{ij} \neq 0$, if the system size is infinite.

Following Ref.²³, let us consider that the $(1,0,0)$, $(0,1,0)$, and $(0,0,1)$ vortices are placed at the edges (P_1, P_2 , and P_3 , respectively) of a triangle, as shown in Fig. 2(a). In the large circle, the total configuration is the integer vortex $(1,1,1)$. In other words, the integer vortex has an internal structure made of three fractional vortices. Instead of the $U(1)^3$ generators $(1,0,0)$, $(0,1,0)$, and $(0,0,1)$, let us prepare four linearly dependent generators: the gauge rotation $(1,1,1)$ and three gauge-invariant rotations $(0,-1,1)$, $(1,0,-1)$, and $(-1,1,0)$. In these generators, the winding of the $(1,0,0)$, $(0,1,0)$, and $(0,0,1)$ vortices can be decomposed into

$$P_1 : \quad (1,0,0) = \frac{1}{3}(1,1,1) + 0(0,-1,1) + \frac{1}{3}(1,0,-1) - \frac{1}{3}(-1,1,0),$$

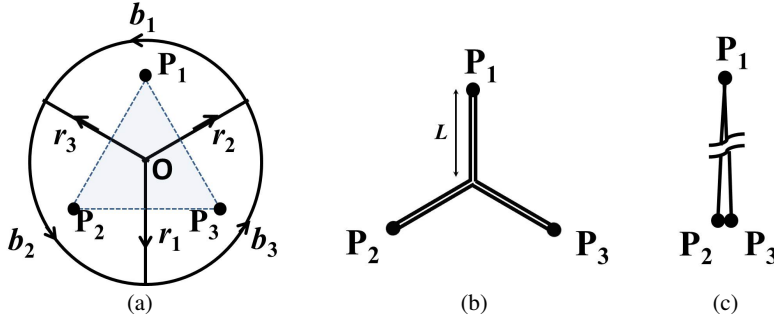


Fig. 2 (a) The $(1,0,0)$, $(0,1,0)$, and $(0,0,1)$ vortices are placed at P_1 , P_2 and P_3 , respectively. b_i ($i = 1, 2, 3$) corresponds to $1/3$ circles at the boundary, and r_i corresponds to the radial paths from the origin O to the circle at the boundary. The $(1,0,0)$, $(0,1,0)$, and $(0,0,1)$ vortices are encircled by $b_1 - r_3 + r_2$, $b_2 - r_1 + r_3$, and $b_3 - r_2 + r_1$, respectively. (b) A domain wall junction. (c) The two vortices P_2 $(0,1,0)$ and P_3 $(0,0,1)$ together are placed at the same position very far from the vortex P_1 $(1,0,0)$. They are connected by a sine-Gordon domain wall.

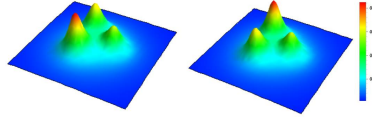


Fig. 3 Two trimers in a three-component BEC ($g_{11} \neq g_{22} \neq g_{33} \neq g_{11}$). The left panel is a mirror image of the right panel.

$$\begin{aligned}
 P_2 : \quad (0, 1, 0) &= \frac{1}{3}(1, 1, 1) - \frac{1}{3}(0, -1, 1) + 0(1, 0, -1) + \frac{1}{3}(-1, 1, 0), \\
 P_3 : \quad (0, 0, 1) &= \frac{1}{3}(1, 1, 1) + \frac{1}{3}(0, -1, 1) - \frac{1}{3}(1, 0, -1) + 0(-1, 1, 0). \quad (9)
 \end{aligned}$$

We see that all b_i ($i = 1, 2, 3$) correspond to $2\pi/3$ rotation of the gauge generator $(1, 1, 1)$, and consequently that these vortices have $1/3$ quantized circulations $h/3m$ for $v_1 = v_2 = v_3$. The $(1, 0, 0)$, $(0, 1, 0)$, and $(0, 0, 1)$ vortices are encircled by $b_1 - r_3 + r_2$, $b_2 - r_1 + r_3$, and $b_3 - r_2 + r_1$, respectively (Fig. 2). Therefore, we can identify the paths $\pm r_1$, $\pm r_2$ and $\pm r_3$ corresponding to $\pm 2\pi/3$ of the phase rotations by $(0, -1, 1)$, $(1, 0, -1)$, and $(-1, 1, 0)$, respectively. The phase rotation along the radial path r_i can be written up to constant phases as

$$\begin{aligned}
 r_1 : \quad \Psi_1 &= |\Psi_1|, \quad \Psi_2 = e^{-(2\pi i/3)f(r)} |\Psi_2|, \quad \Psi_3 = e^{(2\pi i/3)f(r)} |\Psi_3|, \\
 r_2 : \quad \Psi_1 &= e^{(2\pi i/3)f(r)} |\Psi_1|, \quad \Psi_2 = |\Psi_2|, \quad \Psi_3 = e^{-(2\pi i/3)f(r)} |\Psi_3|, \\
 r_3 : \quad \Psi_1 &= e^{-(2\pi i/3)f(r)} |\Psi_1|, \quad \Psi_2 = e^{(2\pi i/3)f(r)} |\Psi_2|, \quad \Psi_3 = |\Psi_3|, \quad (10)
 \end{aligned}$$

where a function $f(r)$ has the boundary conditions $f(r=0) = 1$ and $f(r \rightarrow \infty) = 0$. Since the potential term does not vanish at the origin O , the domain walls cannot connect straight two among P_1 , P_2 and P_3 . We then expect that the three domain walls are bent to constitute a domain wall junction as in Fig. 2(b). Each leg of the junction is a sine-Gordon domain wall. This can be justified if we separate one of

vortices, say P_1 , far from the others as in Fig. 2(c). In the limit that P_1 is separated infinitely, we have $\theta_2 = \theta_3$, and the truncated energy functional (4) for $N = 3$ is reduced to $\mathcal{E}_{\text{phase}}^e = \sum_{i=1}^3 \frac{\hbar^2}{2m} (\nabla \theta_i)^2 - 2v_1 (\omega_{12}v_2 + \omega_{13}v_3) \cos(\theta_1 - \theta_2)$.

Vortex trimers exhibit two new properties that the dimers do not have. The first reported in Ref. ¹⁵ is that the shape of the triangle can be changed by tuning the parameters in Eq. (1). The second is the chirality of the triangle. This can be easily seen when the coupling constants are generic, so that the vortices have different sizes, as seen in Fig. 3. As shown in Fig. 3, the left and right configurations cannot be transformed to each other by a rotation but can be transformed by a mirror. They are energetically completely degenerate.

3.4 Vortex tetramers and N -omers

In multi-component BECs with more than four condensate wave functions, the number of possible molecules increases exponentially. Therefore, in order to classify such vortex molecules, we make use of the mathematical graph theory, in which vortices are expressed by vertices and the Rabi couplings are expressed by edges. Graphs isomorphic to each other are not distinguished in the graph theory. The number of independent connected graphs relevant for four-component BECs is six. In the graph theory, a graph is characterized by the sequence of the number of edges connected to each vertex. For instance, (1, 1, 2, 2) implies that two vertices are connected by two edges, and other two vertices are connected by one edge. We obtained numerical solutions for a four-component BEC with the same values of Rabi couplings (Fig. 4), exhausting all possible graphs with four vortices as vertices including six connected graphs seen in Fig. 4 and two disconnected graphs in Fig. 5. The GP energy (1) subtracted by the ground state energy for each configuration is shown at the top-right of each panel in Fig. 4 and 5, where we chose $r = 6$ for the spatial integration in Eq. (1).

Our simulation indicate the occurrence of several new phenomena that do not exist in dimers or trimers: 1) twist, 2) holding, and 3) capture. We have found that most molecules are accompanied by “twisted” molecules, as in Fig. 4 (a)–(e). A pair of untwisted and twisted molecules corresponds to identical graphs isomorphic to each other, while both pairs are energetically stable, corresponding to absolute (left) and local (right) minima. Once a twisted vortex molecule is formed, a certain amount of finite energy is required to “untwist” it. The holding phenomenon and the absorption of a molecule inside a bigger molecule can be seen in Fig. 5 (a) and (b), respectively.

We can engineer as many multiple vortex molecules as we want with the constituent vortices. As an example, we presented vortex pentamers corresponding to all possible connected graphs with five vertices in a five-component BEC with the same Rabi couplings in Ref. ¹⁶.

Thus far, we have concentrated on the case when $\omega_{ij} = \omega \neq 0$ and $\omega_{ij} = 0$ for the connected and disconnected pair of the vortices, respectively. We can control the positions and shape of the molecule by varying ω_{ij} inhomogeneously. As an example, we present a vortex heptamer (seven vortices), designed as the orion in Fig. 6.

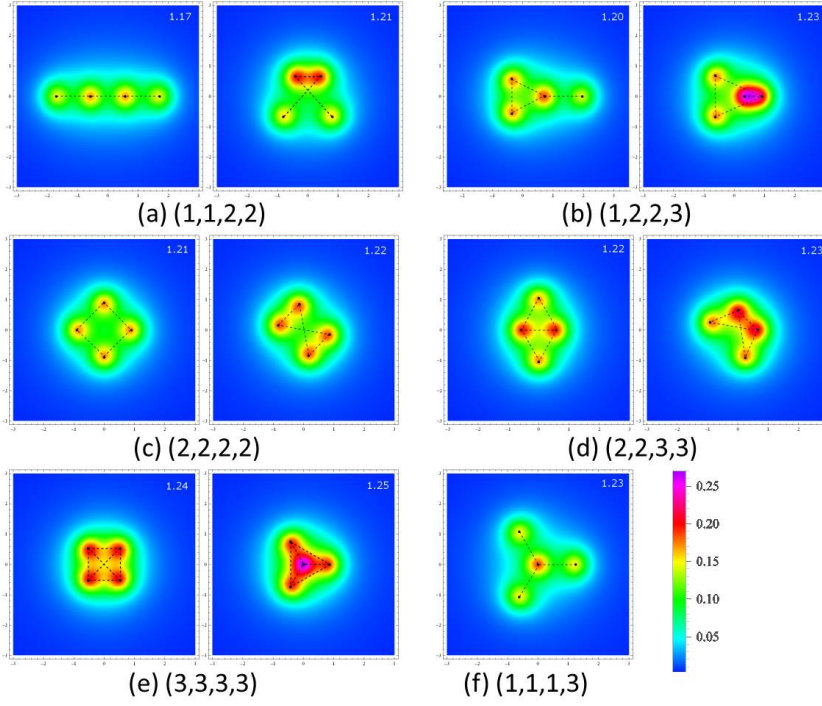


Fig. 4 All possible connected tetramers in a four-component BEC. We set $m = \hbar = 1$, $g = 10^3$, $\tilde{g} = 900$, and $\mu = 10^2$. We also set $\omega_{ij} = 0.05$ and $\omega_{ij} = 0$ for the connected and disconnected pairs, respectively. The dots and dotted lines indicate the vortex center of each component and the Rabi couplings between components, respectively. The color maps represent the energy density. The number at the upper-right corner in each subfigure represents the total energy. For (a), (b), (c), (d) and (e), we have found the stable configurations (the left) and the metastable configurations (the right).

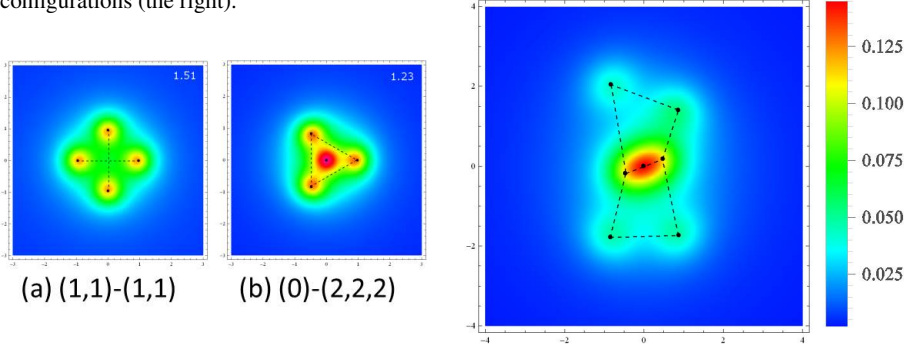


Fig. 5 Disconnected tetramers in a four-component BEC. The parameters are the same with Fig. 4.

Fig. 6 A vortex heptamer designed to be the orion in a seven component BEC. We set $(\omega_{12}, \omega_{23}, \omega_{34}, \omega_{45}, \omega_{16}, \omega_{56}, \omega_{37}, \omega_{67}) = (0.02, 0.001, 0.02, 0.02, 0.05, 0.02, 0.2, 0.2)$ and the rests to be zero.

4 Multiple vortex molecules

So far, we have discussed one integer vortex split into a molecule of fractional vortices. In this section, let us discuss multiple integer vortices. Vortices repel each other so that they can be stable under a rotation. We consider a rotating system $\Omega \neq 0$ with the trapping potential $V_{\text{ex}} = m\omega_{\perp}^2 r^2$.

4.1 Two components

First, let us make comments on the cases without the Rabi couplings. For a few vortices in two-component BECs, vortex pairs constitute vortex polygons²⁴. Vortex polygons have been found to be stable up to five molecules constituting a decagon and metastable for six molecules constituting a dodecagon. However, seven or more molecules are unstable. Polygons of vortex molecules have been also found in field theory²⁵.

For more than six molecules in two component BECs, the ground states are vortex lattice^{6,7,9,12,13,14}. The phase diagram of the vortex lattice forming in the condensate was studied in Refs.^{6,7} and a rich variety of lattices was found. The structure of the two component lattice depends on the sign and on the ratio $g_{12}/g \equiv \delta$ of the coupling constant of the inter/intra-component interactions. When $\delta < 0$, the vortices of different components are attracted and are combined into integer vortices. Because of repulsion among them, they organize in a triangular Abrikosov lattice. If $\delta > 0$, depending on the value of δ and Ω , vortices in each component organize in the triangular lattice, the square lattice, or the vortex-sheet. When $\delta = 0$ the vortices of each component are organized in an Abrikosov lattice, but the vortices of different component are decoupled. If δ is increased, the inter-component interaction results in a repulsive force between the vortices of different components^{11,13} and the two component lattice has a hexagonal structure. When δ is increased further the unitary cell of the single component lattice is changed from a triangle to a square. The value of δ for which the lattice reorganize depends on rotation speed. If $\delta > 1$, phase separation occurs and vortex sheets appear¹⁰. Vortex lattices in two components with different masses were studied in Ref.¹⁴.

So far, the Rabi couplings have not been included in most works on vortex lattices. A systematic study of the internal coherent (Rabi) coupling in vortex lattices in two-component BECs under rotation has been given recently¹⁷. In Fig. 7, we show typical configurations for triangular and square lattices for small Rabi couplings. These vortex lattices must be transformed to the Abrikosov lattice of integer vortices at strong Rabi couplings. In the intermediate Rabi couplings, vortices change their partners in various ways depending on the inter-component coupling to organize themselves for constituting the Abrikosov lattice of integer vortices. Typical examples of the partner changing for a triangular lattice and a square lattice are shown in Fig. 8 (a) and (b), respectively. For the triangular lattice, there exist \mathbb{Z}_3 symmetric equivalent ways. In fact, all patterns appear in the simulation and there appear domain wall defects and a junction.

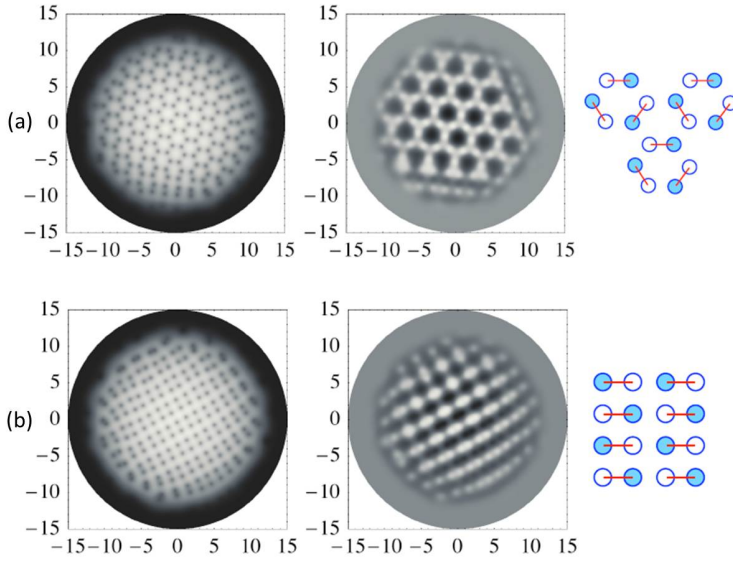


Fig. 7 Vortex lattices with a small Rabi coupling. (a) A triangular lattice and (b) a square lattice. The left panels are plots of the density profile of the condensate, $n = |\Psi_1|^2 + |\Psi_2|^2$ (black dots are vortices in either of the two components), the middle panels are plots of the Rabi energy (white is positive, identified with domain walls), and the right panels are schematic drawings of the lattice structures, where (un)shaded circles denote fractional vortices in first (second) components, and solid lines denote domain walls connecting two fractional vortices.

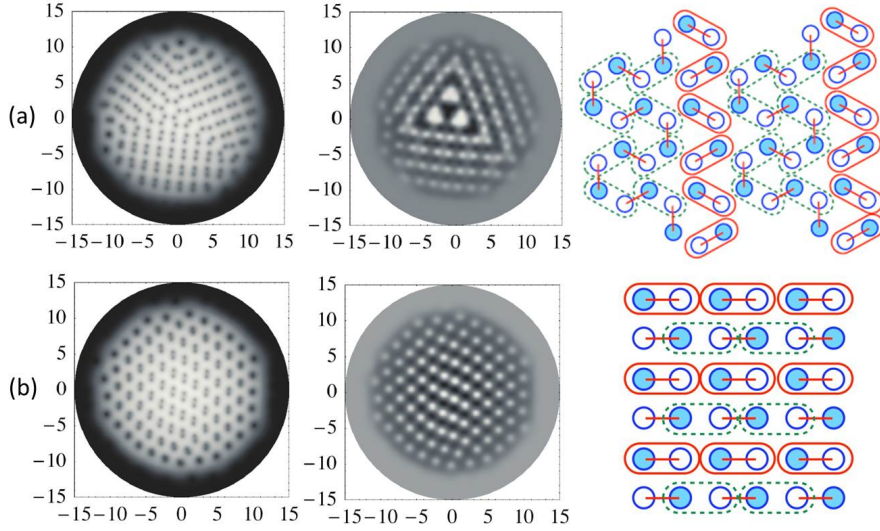


Fig. 8 Partner changing of vortices for (a) a triangular lattice and (b) a square lattice. Notations of the left and the middle panels are the same with Fig. 7. In the right panels, the solid lines indicate the original molecules in Fig. 7, the solid round boxes do not change partners, and the dotted round boxes denote new partners. For the triangular lattice (a), there exist \mathbb{Z}_3 symmetric equivalent ways. In fact, all patterns appear in the simulation and there appear domain wall defects and a junction.

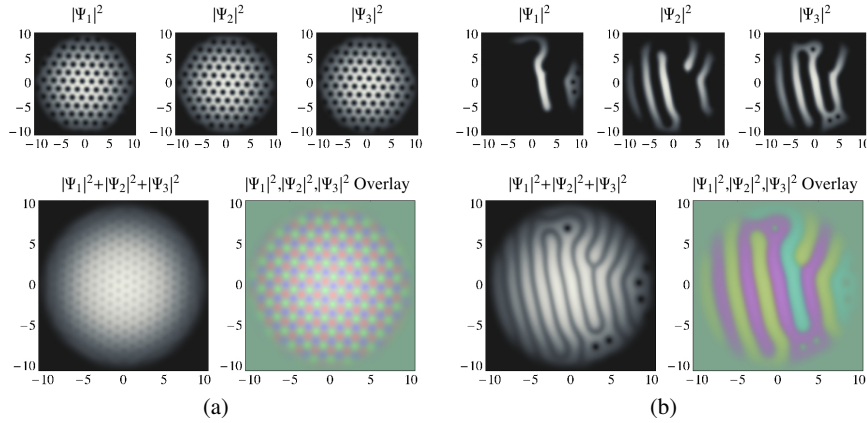


Fig. 9 Vortex lattices (a) and sheets (b) in a three-component BEC. (a) The Abrikosov lattice of $1/3$ quantized vortices for $\delta = 0.5$ (b) Vortex sheets for the phase separated region at $\delta = 1.5$.

4.2 Three components

Vortex lattices in a three-component BEC have been studied recently¹⁸, where three kinds of fractional vortices winding one of three components are present. We have considered the symmetric case where all three intra-component (inter-component) couplings are the same $g_{11} = g_{22} = g_{33} \equiv g$ ($g_{12} = g_{23} = g_{31} \equiv \tilde{g}$) and all chemical potentials and masses are the same as the case of the mixture of atoms with different hyperfine states. Unlike the cases of two-component BECs where the phases of square and triangular lattices are present depending on the intercomponent coupling constant and the rotation speed, we find triangular ordered vortex lattices as in Fig. 9 (a), where three kind of fractional vortices are placed in order without defects, in all parameter region where the inter-component coupling \tilde{g} is less than the intra-component coupling g .

When $g > \tilde{g}$ on the other hand, we find the phase separation as in Fig. 9 (b). In a region where one component is present, the other two components must vanish, where we find ghost vortices in these two components whose positions are separated. We also find a domain wall junction.

The introduction of the Rabi couplings remains as a future problem. However, since the vortex lattices found above are ordered triangular lattices for $\tilde{g} < g$, they will be smoothly connected to the integer Abrikosov lattices with increasing the Rabi couplings.

5 Conclusion

We have reported recent developments of vortex molecules in multi-component BECs. (1) Coherently coupled N -component BECs allow molecules of N fractional vortices connected by sine-Gordon domain walls, representing graphs. (2) Vortex lattices in coherently coupled two-component BECs exhibit a vortex partner changing. (3) Abrikosov vortex lattices are robust in three-component BECs.

Acknowledgements The work of M. N. is supported in part by a Grant-in-Aid for Scientific Research (No. 25400268) and by the “Topological Quantum Phenomena” Grant-in-Aid for Scientific Research on Innovative Areas (No. 25103720) from the Ministry of Education, Culture, Sports, Science and Technology (MEXT) of Japan.

References

1. M. R. Matthews, B. P. Anderson, P. C. Haljan, D. S. Hall, C. E. Wieman, and E. A. Cornell, *Phys. Rev. Lett.* **83**, 2498 (1999).
2. V. Schweikhard, I. Coddington, P. Engels, S. Tung, and E. A. Cornell *Phys. Rev. Lett.* **93**, 210403 (2004).
3. T.-L. Ho, *Phys. Rev. Lett.* **81**, 742-745 (1998); T. Ohmi and K. Machida, *J. Phys. Soc. Jpn.* **67**, 1822 (1998); S. Kobayashi, Y. Kawaguchi, M. Nitta and M. Ueda, *Phys. Rev. A* **86**, 023612 (2012); J. Lovegrove, M. O. Borgh and J. Ruostekoski, *Phys. Rev. A* **86**, 013613 (2012); arXiv:1306.4700.
4. G. W. Semenoff and F. Zhou, *Phys. Rev. Lett.* **98** (2007) 100401; M. Kobayashi, Y. Kawaguchi, M. Nitta and M. Ueda, *Phys. Rev. Lett.* **103** (2009) 115301; Y. Kawaguchi, M. Kobayashi, M. Nitta and M. Ueda, *Prog. Theor. Phys. Suppl.* **186**, 455 (2010).
5. A. M. Turner and E. Demler, *Phys. Rev. B* **79**, 214522 (2009).
6. E. J. Mueller and T.-L. Ho, *Phys. Rev. Lett.* **88**, 180403 (2002).
7. K. Kasamatsu, M. Tsubota and M. Ueda, *Phys. Rev. Lett.* **91**, 150406 (2003).
8. K. Kasamatsu, M. Tsubota and M. Ueda, *Phys. Rev. Lett.* **93**, 250406 (2004).
9. K. Kasamatsu, M. Tsubota and M. Ueda, *Int. J. Mod. Phys. B* **19**, 1835 (2005).
10. K. Kasamatsu, and M. Tsubota, *Phys. Rev. A* **79**, 023606 (2009).
11. M. Eto, K. Kasamatsu, M. Nitta, H. Takeuchi and M. Tsubota, *Phys. Rev. A* **83**, 063603 (2011).
12. P. Mason and A. Aftalion, *Phys. Rev. A* **84**, 033611 (2011).
13. A. Aftalion, P. Mason and W. Juncheng, *Phys. Rev. A* **85**, 033614 (2012).
14. P. Kuopanportti, J. A. M. Huhtamäki, M. Möttönen, *Phys. Rev. A* **85**, 043613 (2012).
15. M. Eto and M. Nitta, *Phys. Rev. A* **85**, 053645 (2012).
16. M. Eto and M. Nitta, arXiv:1303.6048 [cond-mat.quant-gas].
17. M. Cipriani and M. Nitta, arXiv:1303.2592 [cond-mat.quant-gas].
18. M. Cipriani and M. Nitta, *Phys. Rev. A* (to appear) [arXiv:1304.4375]
19. Y. Tanaka, *J. Phys. Soc. Jp.* **70**, 2844 (2001); *Phys. Rev. Lett.* **88**, 017002 (2001).
20. D. T. Son, M. A. Stephanov, *Phys. Rev. A* **65**, 063621 (2002).
21. E. Babaev, *Phys. Rev. Lett.* **89** (2002) 067001; E. Babaev, A. Sudbo and N. W. Ashcroft, *Nature* **431**, 666 (2004); J. Smiseth, E. Smorgrav, E. Babaev and A. Sudbo, *Phys. Rev. B* **71**, 214509 (2005); E. Babaev and N. W. Ashcroft, *Nature Phys.* **3**, 530 (2007).
22. J. Goryo, S. Soma and H. Matsukawa, *Euro Phys. Lett.* **80**, 17002 (2007).
23. M. Nitta, M. Eto, T. Fujimori and K. Ohashi, *J. Phys. Soc. Jap.* **81**, 084711 (2012).
24. M. Kobayashi and M. Nitta, arXiv:1307.1345 [cond-mat.quant-gas].
25. J. Jaykka and M. Speight, *Phys. Rev. D* **82**, 125030 (2010); M. Kobayashi and M. Nitta, *Phys. Rev. D* **87**, 125013 (2013).